

The Apparent “Angular Size – Frequency” Dependence in ~ 3000 Parsec-scale Extragalactic Jets

J. Yang^{1,2}, L.I. Gurvits², S. Frey^{3,4}, and A.P. Lobanov⁵

¹*Shanghai Astronomical Observatory, Chinese Academy of Sciences, 80 Nandan Road, 200030 Shanghai, P.R. China*

²*Joint Institute for VLBI in Europe, PO Box 2, 7990 AA Dwingeloo, The Netherlands*

³*FÖMI Satellite Geodetic Observatory, PO Box 585, 1592 Budapest, Hungary*

⁴*MTA Research Group for Physical Geodesy and Geodynamics, PO Box 91, 1521 Budapest, Hungary*

⁵*Max-Planck-Institut für Radioastronomie, Auf dem Hügel 69, 53121 Bonn, Germany*

ABSTRACT

The upper envelope of the amplitude of the VLBI visibility function usually represents the most compact structural pattern of extragalactic radio sources, in particular, the “core-jet” morphologies. By fitting the envelope to a circular Gaussian model in ~ 3000 parsec-scale core-jet structures, we find that the apparent angular size shows significant power-law dependence on the observing frequency (power index $n = -0.95 \pm 0.37$). The dependence is likely to result from synchrotron self-absorption in the inhomogeneous jet and not the free-free absorption ($n = -2.5$), nor the simple scatter broadening ($n \leq -2$).

Key words: galaxies: active, galaxies: jets, radio continuum: galaxies

1 INTRODUCTION

Radio-loud active galactic nuclei (AGNs) are a class of high-luminosity objects in the Universe. Their pc-scale jets can be well imaged by VLBI observations. The “angular size – frequency” (“ $\theta - \nu$ ”) relation can be used for calibrate the apparent “angular size – redshift” (“ $\theta - z$ ”) relation in which the radio jets are taken as a “standard rod” applicable for testing different cosmological models (Gurvits 2003). The dependence of the size on frequency can provide important constraints for studying the internal physical properties (Lobanov 1998) and the evolution of jets.

An extragalactic radio source generally has a power-law total flux density spectrum resulting from the synchrotron radiation. However, when imaged with VLBI at a milliarc-second resolution, the jet emission often exhibits more complicated spectral shapes, affected by opacity in the emitting material itself and in the surrounding medium. The intervening media along the line of sight scatter/absorb the emission and distort the image, in particular at low (< 1 GHz) frequencies. Thus, the apparent angular size usually depends on the observing frequency. The dependence can be written phenomenologically as a power-law function $\theta \propto \nu^n$ in most cases. For instance, $n = -2$ for the compact radio source at the center of our Galaxy (Sgr A*) as a result of scatter broadening (Shen et al. 2005).

Table 1. Summary of the used data set.

| Band | ν_{obs} (GHz) | R (mas) | N_{source} | Surveys |
|------|-----------------------------|--------------|---------------------|--------------------------------------------|
| S | 2.3 | 3.2 | 3115 | RRFID ^a and VCS ^b |
| C | 5.0 | 1.4 | 1406 | VIBApIs ^c and VIPs ^d |
| X | 8.4 | 0.85 | 3004 | RRFID and VCS |
| Ku | 15 | 0.47 | 299 | VLBA 2-cm Survey |
| Ka | 24 | 0.32 | 264 | RRFID |
| Q | 43 | 0.17 | 124 | RRFID |

Columns: (1) Observing band; (2) Observing frequency; (3) Angular resolution of the VLBA at this band; (4) Number of sources analysed; (5) Major VLBI surveys from which the data are obtained.

^a RRFID: Radio Reference Frame Image Database (Fey & Charlot 2000).

^b VCS: VLBA Calibrator Surveys (Petrov et al. 2006).

^c VIBApIs: VSOP Pre-lunch Survey (Fomalont et al. 2000).

^d VIPs: VLBA Imaging and Polarimetry Survey (Helmboldt et al. 2007).

2 THE CHARACTERISTIC ANGULAR SIZE

The characteristic angular size is a parameter describing the width of the intensity distribution of jet emission. Generally, it can be defined either in the image plane or in the u - v (Fourier) plane. For instance, a measure of the characteristic size can be provided by the distance between the brightest component and the most distant one with the brightness at least 2% of the peak (Kellermann 1993) in the image plane. It is also feasible to obtain the estimated angular size by fitting a circular Gaussian model to the visibility data (Gurvits 1994) in the u - v plane. Although the two ways are equivalent in principle, the definitions in the u - v plane are more

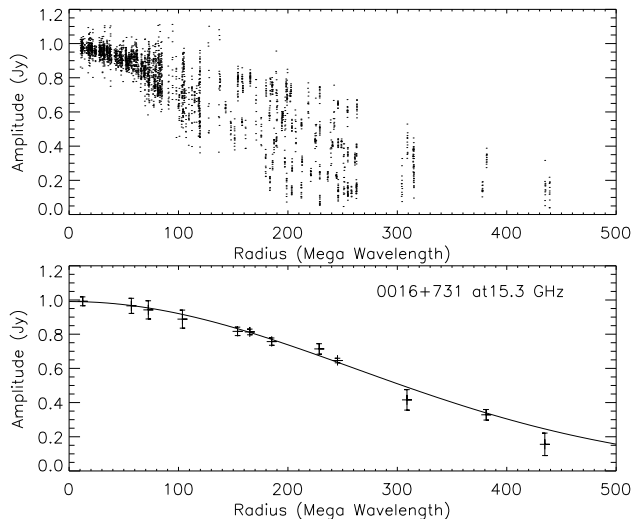


Figure 1. An example for the definition of the characteristic angular size. The top panel shows the original visibility data. The bottom panel shows the extracted upper envelope points and the fitting Gaussian curve.

direct than those in the image plane, and free from sampling effect. If the visibility data have enough sensitivity, the “super-resolution” can be obtained for the barely resolved sources using a certain model (Lobanov 2005). Here we define the characteristic angular size θ by fitting the upper envelope of the visibility amplitudes to a circular Gaussian model (Pearson 1999):

$$\Gamma(\rho) = \exp \left[\frac{-(\pi\theta\rho)^2}{4 \ln 2} \right] \quad (1)$$

where θ is the full width to half-maximum intensity (FWHM) in the image plane in radian, ρ is u - v radius in wavelength and $\Gamma(\rho)$ is the normalized amplitude. The characteristic angular size represents the most compact and the brightest part of the source. Fig. 1 gives an example for the definition of the characteristic angular size.

3 DATA COLLECTION

Table 1 gives a brief summary of our data set of 4000 objects compiled from several large VLBI surveys (see references in Frey 2006). Some sources have multi-frequency and/or multi-epoch observations. All the visibility data have been calibrated, self-calibrated, and saved as standard u - v FITS files. We developed several programs to automatically calculate the characteristic angular size according to our definition using the IDL Astronomy Users Library. We extracted the upper envelope points from the original visibility data, fitted them by a circular Gaussian model, and finally fitted the “ $\theta - \nu$ ” data to a power-law function to determine the power index n for the multi-frequency observations.

4 RESULTS

Fig. 2 shows the statistical distributions of the characteristic angular sizes. The histograms show a similar shape peaking

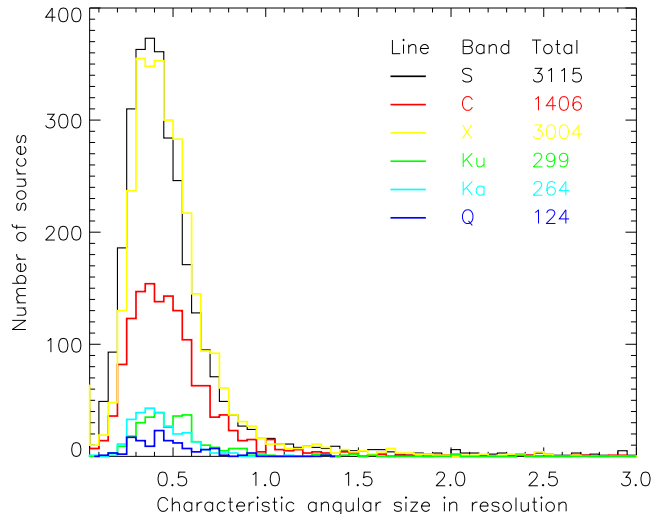


Figure 2. The statistical distributions of the characteristic angular sizes. Different colors represent different bands. Note that the angular size is expressed in units of the resolution of the VLBA array at each band.

at the position of $\sim 0.4R$, where R is the resolution of the VLBA array at each band and listed in Column 3, Table 1. The Ku-band distribution is consistent with the previous results in the MOJAVE sample by Kovalev et al. (2005). They fitted the core by an elliptical Gaussian model in Difmap. Fig. 3 shows the distribution of the power index n , which has a mean value of -0.95 ± 0.37 for 2827 sources with at least two-frequency observations and -0.96 ± 0.21 for 315 sources with at least four-frequency observations. The dependence agrees well with the results from fitting the core by an elliptical Gaussian model in 167 objects (Jiang et al. 2001). Note that we assume that the power index n is independent of redshift within the studied range of redshift ($0 < z < 5$).

5 DISCUSSION

The upper envelope statistically gives the size of the brightest and most compact component. Among all the components in a pc-scale jet, the core/jet base usually has a flatter spectrum and dominates the total flux density. Thus, the upper envelope gives the size of the radio core in most cases.

The radio core generally has a flat spectrum and is located in the region where the optical depth $\tau = 1$. Königl (1981) demonstrated that, due to the synchrotron self-absorption, the size of the core r_{core} varies with the frequency ν as: $r_{\text{core}} \propto \nu^{-1/k_r}$, where k_r depends on the shape of the electron energy spectrum and on the distribution of the magnetic field and particle density in an inhomogeneous jet, $k_r = 1$ in the case of the equipartition between jet particle and magnetic field energy densities (Lobanov 1998). Our results agree well with this prediction.

Free-free absorption by the plasma covering the jet also results in an optically thick core. However, free-free absorption is only found in a few sources. Lobanov (1998) suggested that the shift of core position is $r_{\text{core}} \propto \nu^{-2.5}$ for a spherical distribution of free-free absorption plasma $N_e \propto r^{-3}$, where r is the distance from the center and N_e is the electron number density. So, the free-free absorption is not the

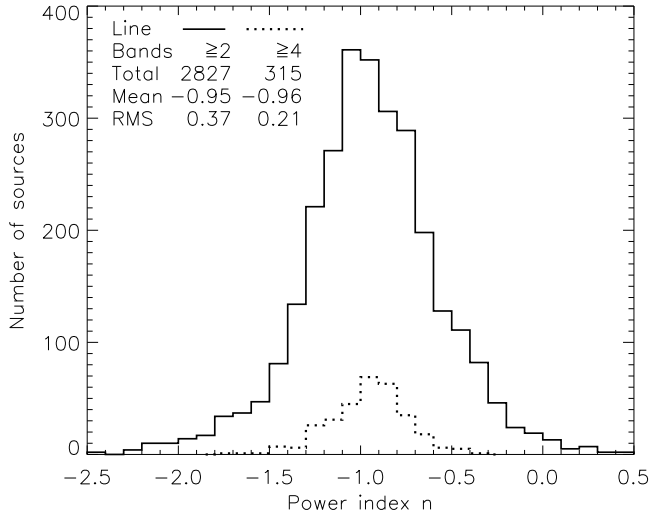


Figure 3. The statistical distribution of the power index n . The solid line represents the result from all the sources with at least two-frequency observations. The dotted line represents the result from all the sources with at least four-frequency observations.

right mechanism to explain the statistical relation presented here. It might however happen in some sources. As far as the simple diffractive scattering models, e.g. the Gaussian screen model or the power-law model with the Kolmogorov spectrum, are concerned, they result in a dependence with $n \leq -2$ (Thompson et al. 1986), which is fairly far from the peak ($n \sim -0.9$) of the obtained distribution. Thus, simple scatter broadening cannot explain the dependence.

6 CONCLUSIONS

Based on the above discussion, we can draw the following conclusions.

- (i) The upper envelope of visibility amplitudes is a statistically meaningful characteristic angular size for the radio “core”.
- (ii) The apparent “angular size – frequency” dependence can be statistically described by $\theta \propto \nu^{-0.95 \pm 0.37}$ in ~ 3000 pc-scale jets.
- (iii) The observed frequency dependence can be explained as a result of synchrotron self-absorption in the inhomogeneous jet. The simple scatter broadening and free-free absorption can be ruled out as dominant mechanisms responsible for the dependence.

7 ACKNOWLEDGMENT

J. Yang is grateful to the KNAW-CAS grant 07DP010. S. Frey acknowledges the OTKA K72515 grant. We made use of the collection of calibrated VLBI u - v data maintained by L. Petrov at NASA Goddard Space Flight Center (GSFC). This research has made use of NASA’s Astrophysics Data System, NASA/IPAC Extragalactic Database (NED) and the United States Naval Observatory (USNO) Radio Reference Frame Image Database (RRFID). We thank A.L. Fey for providing the RRFID data. The National

Radio Astronomy Observatory is a facility of the National Science Foundation operated under cooperative agreement by associated Universities, Inc.

REFERENCES

- Fey A.L., Charlot P., 2000, ApJS 128, 17
- Fomalont E.B., et al., 2000, ApJS 131, 95
- Frey S., 2006, in Proceedings of the 8th European VLBI Network Symposium, ed. Marecki A. et al., Proceeding of Science, PoS(8thEVN)001
- Gurvits L.I., 1994, ApJ 425, 442
- Gurvits L.I., 2003, in Radio Astronomy at the Fringe, ed. Zensus J.A., et al., ASP Conference Series 300, 285
- Helmholtz J.F., et al. 2007, ApJ 658, 203
- Jiang D.R., et al., 2001, in Galaxies and their Constituents at the Highest Angular Resolutions, ed. Schilizzi R.T., et al., IAU Symposium 205, 148
- Kellermann K.I., 1993, Nature 361, 134
- Kovalev Y.Y., et al., 2005, AJ 130, 2473
- Lobanov A.P., 1998, A&A 330, 79
- Lobanov A.P., 2005, astro-ph/0503225
- Pearson T.J., 1999, in Synthesis Imaging in Radio Astronomy II, Taylor G.B., et al., ASP Conference Series, 180, 335
- Petrov L., et al., 2006, AJ 131, 1872
- Shen Z.-Q., et al., 2005, Nature 438, 62
- Thompson A.R., et al., 1986, Interferometry and Synthesis in Radio Astronomy (New York: Wiley)